RESEARCH ARTICLE

Finite-Element Analysis of a Novel Cephalomedullary Nail for Restricted Sliding to Reduce Risk of Implant Failure in Unstable Intertrochanteric Fractures

Shaobo Nie, PhD[1,2†], Jiantao Li, PhD[1,2†], Ming Li, PhD[1,2†], Ming Hao, PhD[1,2], Kun Wang, PhD[1,2], Ying Xiong, PhD[3], Xuewen Gan, PhD[3], Licheng Zhang, PhD[1,2] ⓘD, Peifu Tang, PhD[1,2] ⓘD

[1]Department of Orthopedics, PLA General Hospital and [2]National Clinical Research Center for Orthopedics, Sports Medicine & Rehabilitation, Beijing and [3]Department of orthopedics, Yan'an Hospital Affiliated to Kunming Medical University, Kunming, China

Objective: How to restrict sliding of cephalomedullary nail and rigid reconstruct medial support for unstable intertrochanteric fractures remains a challenge. This study aims to explore the feasibility of a novel cephalomedullary nail for restriction sliding and reconstruction of medial femoral support to prevent failure in unstable trochanteric fractures through finite element analysis.

Methods: The DICOM files of a unilateral femur spiral computed tomography (CT) scans from a elderly female were converted into STL files, and the most common clinical trochanteric fracture model with the absence of medial support, AO/OTA 31-A2.3 was simulated by removing the posterior medial femur. The model of a novel medial sustain nail (MSN-II) and a widely used nail (proximal femoral nail anti-rotation PFNA-II) were modeled according to the manufacturer-provided engineering drawing. Different loads were applied to the femoral head to simulate the postoperative weight bearing gait. The sliding distance of helical blade in femoral neck, maximum stress of femur and nail, displacement of proximal fragment were analyzed to revealing the mechanical stability of unstable trochanteric fracture stabilized by different implant.

Results: The sliding distance of helical blade in the femoral neck, the maximum stress on the femur and nail, the displacement of proximal fragment in MSN-II under 2100N axial load were 0.65 mm, 689 MPa, 1271 MPa, 16.84 mm respectively, while that were 1.43 mm, 720.8 MPa, 1444 MPa, 18.18 mm, respectively in PFNA-II. The difference between the two groups was statistically significant ($P < 0.05$) and the stress was mainly distributed in medial distal side of nail but helical blade and the proximal aperture for the nail in MSN-II. Compared to PFNA-II, MSN-II demonstrates biomechanical merit against femur medialization, cut-out and coax varus.

Conclusion: The sliding distance of helical blade in femoral neck, the maximum stress on the femur and nail, and the displacement of proximal fragment of MSN-II were less than those of PFNA-II in the treatment of unstable intertrochanteric fractures. Therefore MSN-II has better stability than PFNA-II and it may have the potential to avoid femur medialization and cut out. It might be an option in unstable trochanteric fracture because of its superiority in restricted sliding and medial support reconstruction.

Key words: Finite element analysis; Medial support; Proximal femoral nail anti-rotation; Sliding; Unstable trochanteric fracture

Introduction

The incidence of hip fractures is predicted to rise by 12% from 2010 to 2030,[1] and more than 50% of it will occur in Asia by 2050.[2] More than half of hip fractures are trochanteric fractures in older patients, with 1 year mortality rate up to 36% because of immobilization,[3] so surgical stabilization and early mobilization is the keystone in the treatment. Cephalomedullary nailing is the mainstream in trochanteric fractures, especially for unstable fractures, as its axial fixation and the ability of earlier weight bearing.[4] But the implant failure has been reported as high as 22.3%,[5] that mainly due to the mechanical conduction structure of the medial femur cannot be reconstructed after the unstable trochanteric fractures[6] and the excessive sliding or femoral medialization.[7]

Restoring medial cortical support is important in unstable intertrochanteric fractures but is often difficult to achieve in clinical practice. The comminuted trochanteric fractures (especially AO/OTA 31-A2.3) account for more than 80% of unstable trochanteric fractures,[8] which are the main component of implant failure. Comminuted medial wall fractures are difficult to maintain reduction due to the muscle traction. Moreover, the proximal femur is prone to loss of reduction and implant failure due to swing effect[9] when it is fixed by cephalomedullary nail as the wide medullary cavity caused by osteoporosis and the advanced age.[10] Chen et al. reported that the postoperative reduction loss rate due to comminuted medial wall was as high as 20%.[11] Song et al. found that calcar fracture gapping (comminuted medial wall) is a reliable predictor of implant failure after cephalomedullary nailing for trochanteric fractures.[12] None of the existing cephalomedullary nails can effectively reconstruct the medial femoral support.[13] Therefore, reconstruction and maintenance of medial femoral cortical support is a key factor in reducing the risk of implant failure and seems unavoidable as confirmed in our previous research.[6]

Dynamic sliding implants such as Dynamic Hip Screw (DHS) or Proximal Femoral Nail Anti-rotation (PFNA-II) is the golden standard in trochanteric fractures as it did yield a lower risk of unplanned return to theater.[14] However, excessive sliding or femoral medialization of those implants is a risk factor for implant failure[15] and is a unique complication that occurs almost exclusively in the treatment of unstable trochanteric fractures with cephalomedullary nailing.[16] Law et al. found that intramedullary nailing of unstable intertrochanteric fractures is inherently predisposed to femoral neck element medial migration making it more susceptible to consequent cut-out compared to fixation with the DHS.[17] A large number of studies have confirmed that excessive sliding may lead to implant-related complications such as cut-out, which contributes significantly to the overall failure rate of implants.[18] In order to limit the excessive sliding, non-cylindrical and more blade-like head fixation devices have been developed to prevent, or at least reduce, the failure rate in the latest implant generation.[19] But excessive sliding is reported as sliding of ≥8mm, which occurs in approximately 40% of cases.[20]

Some techniques are available to enhance cephalomedullary nailing for unstable trochanteric fractures to reduce the risk of implant failure by restoring mechanical conduction of the medial femur and limiting excessive sliding.[21] Cerclage cable is the most common medial support reconstruction technique in cephalomedullary nailing for trochanteric fractures,[22] but whether cerclage can improve fixation is still controversial.[23,24] Ceynowa et al. confirmed that medial wall reconstruction with a cerclage cable does not improve axial stability of the fixation through biomechanical study.[25] Cement augmentation for trochanteric fractures is considered viable to limit the excessive sliding by enhancing the implant anchorage within the head and neck fragment and lead to promote patient early mobilization.[26] However, evidence regarding the effect of cement augmentation on fixation failures was very uncertain. Cement augmentation did not reduce the risk of loss of reduction, implant loosening and malunion.[27] However, catastrophic leakage complications are another reason for caution. To our best knowledge, restoring medial support and limiting excessive sliding are still pending problems in the treatment of intertrochanteric fractures.

The theory of triangular stability[28] was proposed based on the triangular-stable mechanical in the proximal femur in our earlier study and a novel medial sustain nail (Medial Sustain Nail-MSN, Fig. 1A) was designed by that which could restored the triangular-stable mechanical in the proximal femur by reconstructed the femoral medial support. It was found that MSN was superior to PFNA-II in reducing displacement and anti-rotation performance in early biomechanical tests,[29] however, the defect of excessive sliding of helical blade still exists. The design of MSN was improved by adding a limited slide groove and changing the structure of the helical blade (MSN-II, Fig. 1B), and satisfactory results of medial support reconstruction were confirmed by biomechanics.[30] It is not clear whether the excessive sliding is restricted. The aim of this study was to determine by finite element analysis: (i)whether the novel nail can reduce risk of cut out by restriction sliding? (ii) whether the novel nail can reduce risk of coxa varus by reconstructing the medial support? And (iii) whether the novel nail has potential risks?

Materials and Methods

Materials and Subjects

A healthy elderly female, 160 cm in height, 70 kg in weight and 70 years old, underwent a CT scan with a slice thickness of 1mm of the femur after examination to rule out hip disease and deformity but osteoporosis. This 3D finite element model has been used in a previous study.[31]

This study was approved by the ethics committee of the PLA General Hospital and written informed consent was obtained from a healthy volunteer(S2020-114-04).

FINITE-ELEMENT ANALYSIS OF A NOVEL CEPHALOMEDULLARY NAIL IN UNSTABLE INTERTROCHANTERIC FRACTURES
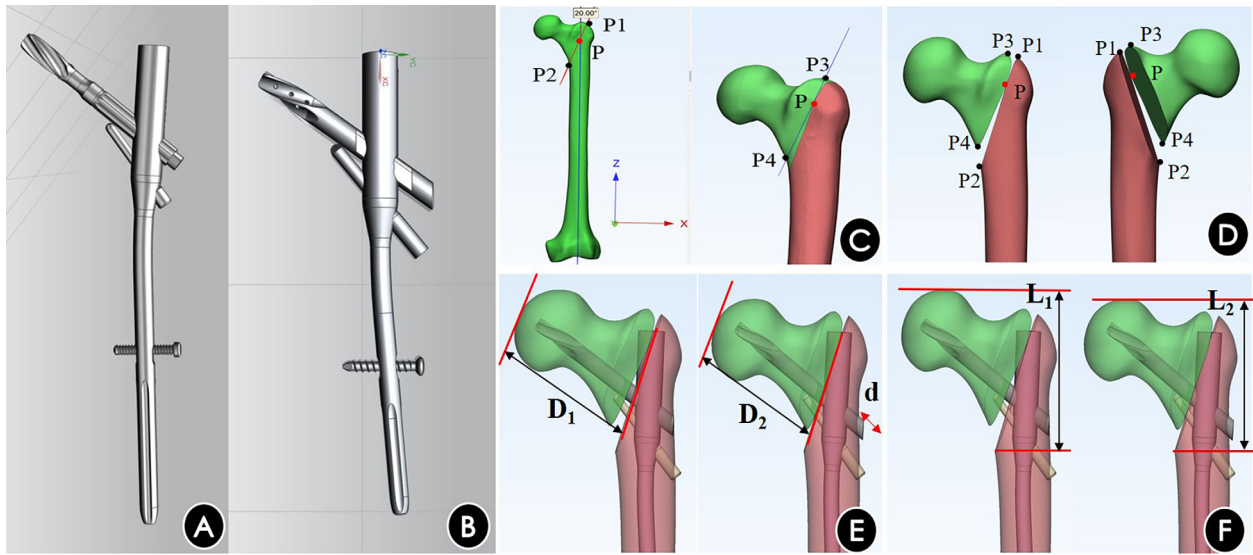
Fig. 1 Model of unstable intertrochanteric fracture and implant. (A) Schematic diagram of MSN-I. (B) Schematic diagram of MSN-II. (C) Schematic diagram of the first and second simulated osteotomy line. P is the rotation point, P1 is the intersection point between the first osteotomy line and the greater trochanter, and P2 is located at the lower level of the lesser trochanter. P3 is the apex of the greater trochanter after femoral shaft internal rotation, and P4 is located at the upper level of the lesser trochanter after femoral shaft internal rotation. (D) Model of unstable intertrochanteric fracture without medial support (AO/OTA 31-A2.3) (Front view on the left, back view on the right). (E) Method for measuring sliding distance of helical blade in femoral neck (Sliding distance = (D₁-D₂)-d, D₁ is the vertical distance from the femoral head to the osteotomy plane of the distal femur before loading and D2 is the distance after loading. d is the length difference of the helical blade tail outside the bone cortex before and after loading). (F) Method for measuring displacement of proximal fragment (displacement of proximal fragment = L₁-L₂. L₁ is the distance from the femoral head to the medial side of the distal osteotomy line before loading and the L₂ is the distance after loading)

Methods

Model Establishment

The DICOM data of the full length of the left femur (unilateral femur) from CT were imported into Mimics 16.0 software (Materialise, Leuven, Belgium), and the coronal plane, sagittal plane and horizontal plane were defined respectively to reconstruct the femoral model. Cortical bone and cancellous bone were modeled as two separate sections. With the method of dynamic region growth of software, the human bone threshold value was selected, and the femur model was established, that was saved as a binary STL format file. The file was imported into Geomagic 12.0 (Geomagic co, Cary, NC, USA) for surface construction. The burrs and voids were repaired and then the surface triangular patches were repaired, and noise reduced to realize the smoothing of the femoral model. A standardized posteromedial unsupported intertrochanteric fracture (AO-A2.3; the most unstable and most common type in comminuted trochanteric fracture) was created by two simulated fracture line[32] and has been used in the previous studies.[29] The anatomical axial of femoral shaft was established in 3-Matic 12.0 (Materialise NV, Leuven, Belgium). And a plane through the femoral axis that was perpendicular to the XZ-plane of the world coordinate system (WCS) was obtained. Then the plane was rotated 20° clockwise around Y-axis of the WCS through the rotation center of red point (P in Fig. 1C) on the trochanteric anterior cortex. So we got the first osteotomy plane. Then we created second osteotomy plane which was determined by three points: P point, the apex of the greater trochanter (P3 in Fig. 1C,D), and the upper end of the less trochanter (P4 in Fig. 1C,D). The intertrochanteric crest and the lesser trochanter between the two osteotomy lines were completely removed, and part of greater trochanter, especially the posterior part, was removed. The models of implant (MSN-II and PFNA-II) were modeled by UG 8.5 (Siemens, Saint Paul, MN, USA) according to the manufacturer-provided engineering drawing. Assemblage of the implants and the posteromedial unsupported intertrochanteric fracture models were accomplished in 3-matic. The helical blades were located in the middle and lower third of the femoral neck. The entry point was located at the apex of the greater trochanteric in anteroposterior radiographic fluoroscopy and the extension of the femoral shaft in lateral. Parameters of PFNA-II were as follows: nail length 240mm with proximal diameter 16mm and distal diameter 10mm, helical blade length 110mm with the diameter 9.9mm and spiral blade length 30mm, distal lock screw length 45mm with diameter

4.9mm. Parameters of MSN-II were as follows: nail length 240mm with proximal diameter 16mm and distal diameter 10mm, medial support screw length 61.5mm with the diameter 4.9mm, helical blade length 110mm with the diameter 9.9mm and spiral blade length 30mm.

TABLE 1 Parameter of model material

Material	Elasticity modulus	Poisson's ratio
Cortical bone	12.4 GPa	0.3
Cancellous bone	77 MPa	0.3
Titanium alloy	114 MPa	0.28

Fig. 2 Diagram of sliding distance of helical blade in femoral neck in two kinds of implants under different loads

Assignment and Boundary Setting
The surface of the femur was selected as cortical bone with a thickness of 2mm and the remainder as cancellous bone, and HyperMesh 12.0 (Altair, Maple Grove, MN, USA) was used to complete the pre-calculation process, including meshing, definition and assignment.[33]

Boundary conditions were set in Abaqus11.0 (Abaqus, Providence, RI, USA), binding was set between the support nail and the main nail, friction coefficient between fracture blocks was 0.46, friction coefficient between internal fixation was 0.23, and coefficient between bone and internal fixation was 0.3,[34] and the internal fixation was made of titanium alloy. Parameters of internal fixation and femur[31] are listed in Table 1.

Load Settings
The distal femur was set as binding and the axial stress of the model was applied to the femoral head, with the force direction was 10° adduction on the coronal plane and 9° adduction on the sagittal plane.[35] The axial loads were 300N, 600N, 900N, 1200N, 1500N, 1800N, and 2100N, respectively, to simulate the process from partial to complete weight-bearing after surgery,[29,31] and the stress distribution and displacement of femur were recorded.

Assessment Criteria
After the finite element simulation test, the sliding distance of the helical blade in the femoral neck (mm), the maximum stress (MPa) of the femur, the MPa of the implant and the maximum displacement (mm) of the proximal fragment were measured and recorded. The displacement difference
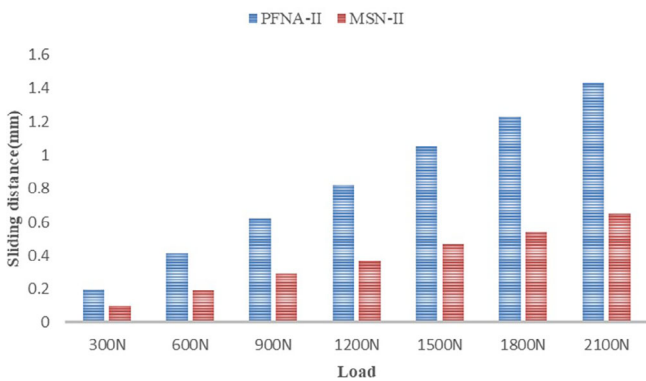

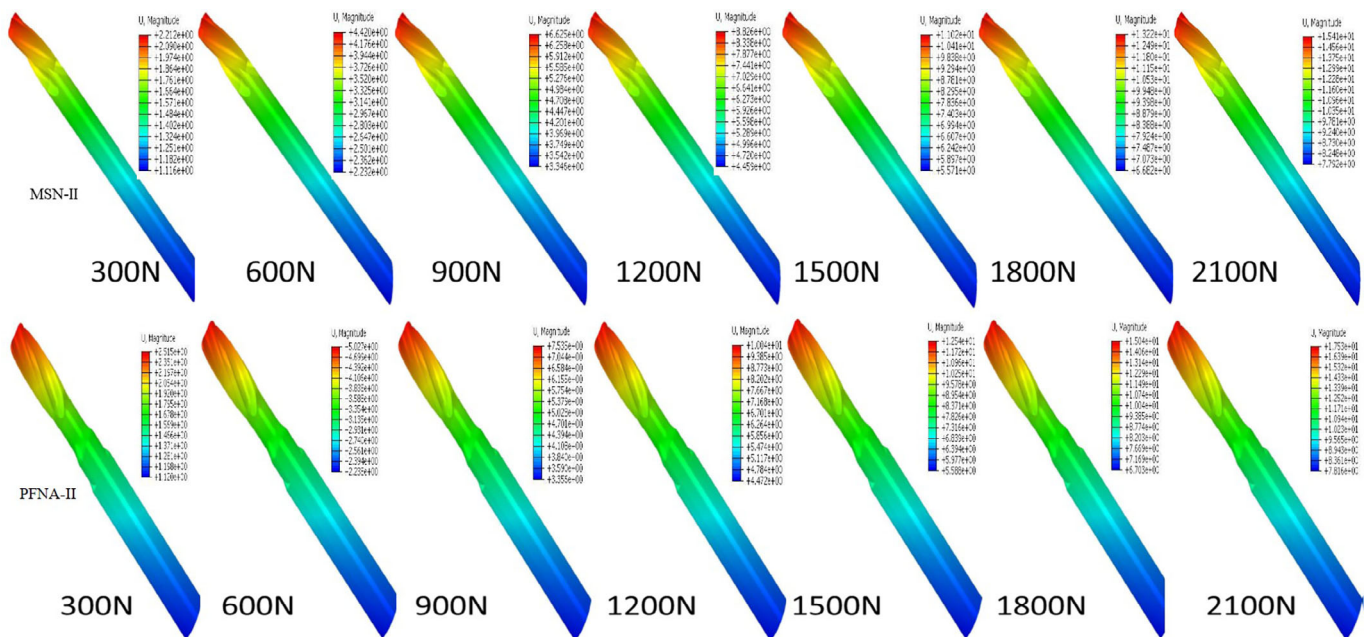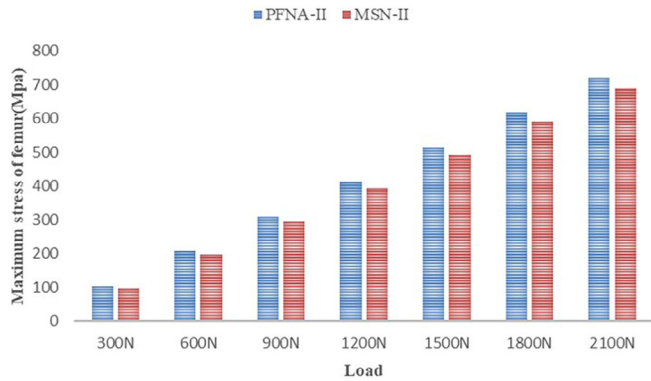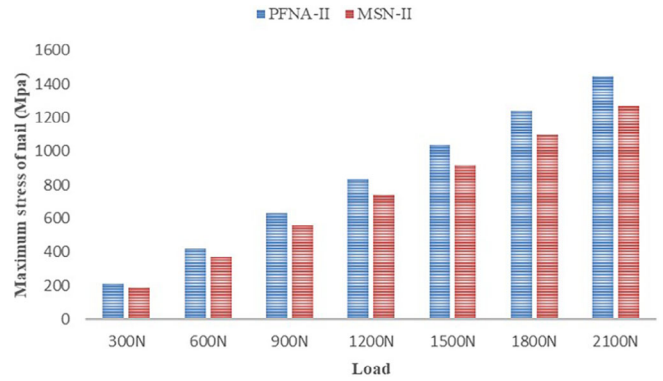**Fig. 3** Pressure cloud diagram of the sliding distance of helical blade in femoral neck in MSN-II and PFNA-II under different loads

Fig. 4 Diagram of the maximum stress of femur in two kinds of implants under different loads

Fig. 6 Diagram of maximum stress on two kinds of nails under different loads

between the proximal fragment and the helical blade on the anatomical axis of the femoral neck was defined as the sliding distance of the helical blade in the femoral neck (Fig. 1E). The maximum stress of the femur was defined as the maximum stress on the femoral head. The maximum stress of the implant was indicated by the maximum stress below the junction between the helical blade and the nail. The displacement difference of the proximal fragment on the coronal plane before and after loading was defined as the maximum displacement of proximal fragment (Fig. 1F).

Statistical Analysis
SPSS 22.0 software (IBM Corp., Armonk, NY, USA) was used for statistical analysis in this study. Finite element analysis data such as sliding distance and maximum stress between MSN-II and PFNA-II were statistically compared

using the paired *t*-test. The significance was measured according to a *P* value of 0.05.

Results

Sliding Distance of Helical Blade in Femoral Neck
Under different loads of 300 N, 600 N, 900 N, 1200 N, 1500 N, 1800 N and 2100 N, the sliding distance of MSN-II and PFNA-II helical blade in femoral neck were 0.1 mm, 0.19 mm, 0.29 mm, 0.37 mm, 0.47 mm, 0.54 mm, 0.65 mm respectively and 0.2 mm, 0.41 mm, 0.62 mm, 0.82 mm, 1.05 mm, 1.23 mm, 1.43 mm respectively. The sliding distance of MSN-II helical blade in femoral neck is less than that of PFNA-II at different loads and the increasing trend of the sliding distance was also significantly smaller than PFNA-II. The sliding distance of helical blade in femoral neck of the two groups under continuous
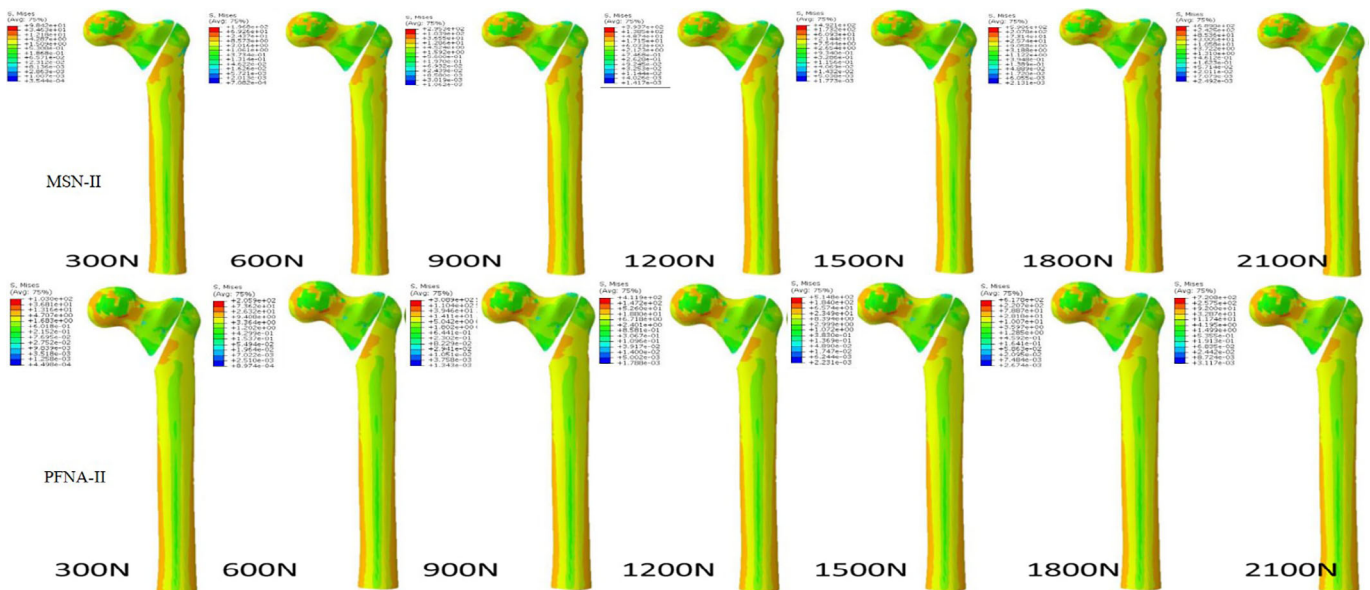
Fig. 5 Pressure cloud diagram of the maximum stress of femur in MSN-II and PFNA-II under different loads
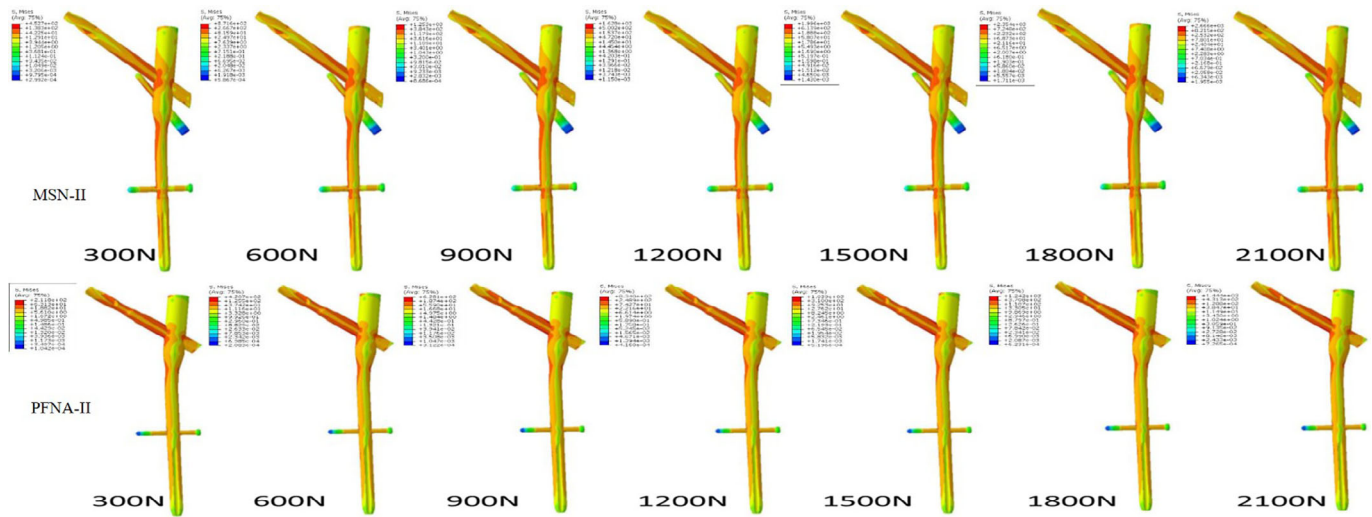
Fig. 7 Pressure cloud diagram of the maximum stress on MSN-II nail and PFNA-II under different loads
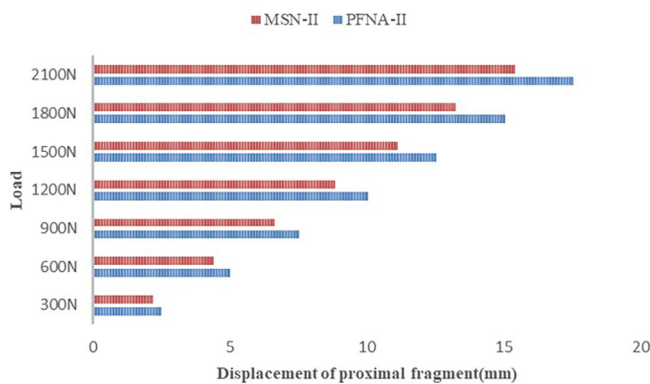
Fig. 8 Diagram of displacement of proximal fragment in two kinds of implants under different loads

increasing axial load is shown in Fig. 2 and the pressure cloud diagram is shown in Fig. 3.

Maximum Stress of Femur
Under different loads of 300 N, 600 N, 900 N, 1200 N, 1500 N, 1800 N and 2100 N, the maximum stress of femur in MSN-II and PFNA-II were 98.4 MPa, 196.8 MPa, 295.3 MPa, 393.7 MPa, 492.1 MPa, 590.6 MPa, 689 MPa respectively and 103 MPa, 205.9 MPa, 308.9 MPa, 411.9 MPa, 514.8 MPa, 617.8 MPa, 720.8 MPa respectively. The increasing trend of the maximum stress of femur in MSN-II was less than that of PFNA-II under different loads. The diagram of that is shown in Fig. 4. The pressure cloud diagram of the two groups is shown in Fig. 5.

Maximum Stress of Nail
Under different loads of 300 N, 600 N, 900 N, 1200 N, 1500 N, 1800 N and 2100 N, the maximum stress of MSN-II and PFNA-II were 187.4 MPa, 373.2 MPa, 557.0 MPa,

738.7 MPa, 918.3 MPa, 1096 MPa, 1271 MPa respectively and 211.8 MPa, 420.7 MPa, 628.1 MPa, 834.0 MPa, 1039 MPa, 1242 MPa, 1444 MPa respectively. The increasing trend of the maximum stress of MSN-II was less than that of PFNA-II under different loads. The maximum stress of the two implants under continuous increasing axial load is shown in Fig. 6 and the pressure cloud diagram is shown in Fig. 7.

Displacement of Proximal Fragment
Under different loads of 300 N, 600 N, 900 N, 1200 N, 1500 N, 1800 N and 2100 N, the displacement of proximal fragment in MSN-II and PFNA-II were 2.41 mm, 4.83 mm, 7.24 mm, 9.64 mm, 12.05 mm, 14.45 mm, 16.84 mm respectively and 2.61 mm, 5.21 mm, 7.81 mm, 10.41 mm, 13.01 mm, 15.6 mm, 18.18 mm respectively. The increasing trend of the displacement of MSN-II was less than that in PFNA-II under different loads. The maximum stress distribution on the femur of the two groups under continuous increasing axial load is shown in Fig. 8 and the pressure cloud diagram is shown in Fig. 9.

Comparison of Biomechanical Characteristics and Statistical Analysis
The sliding distance of helical blade in the MSN-II group decreased by 0.45 mm compared with the PFNA-II group, and the difference was statistically significant ($I = -4.774$, $P < 0.05$). The maximum stress of femur in the MSN-II group decreased by 18.2 MPa compared with the PFNA-II group, and the difference was statistically significant ($I = -4.911$, $P < 0.05$). The maximum stress of nail in the MSN-II group decreased by 18.2 MPa compared with the PFNA-II group, and the difference was statistically significant ($t = -4.796$, $P < 0.05$). The displacement of proximal fragment in the MSN-II group decreased by 0.8 mm
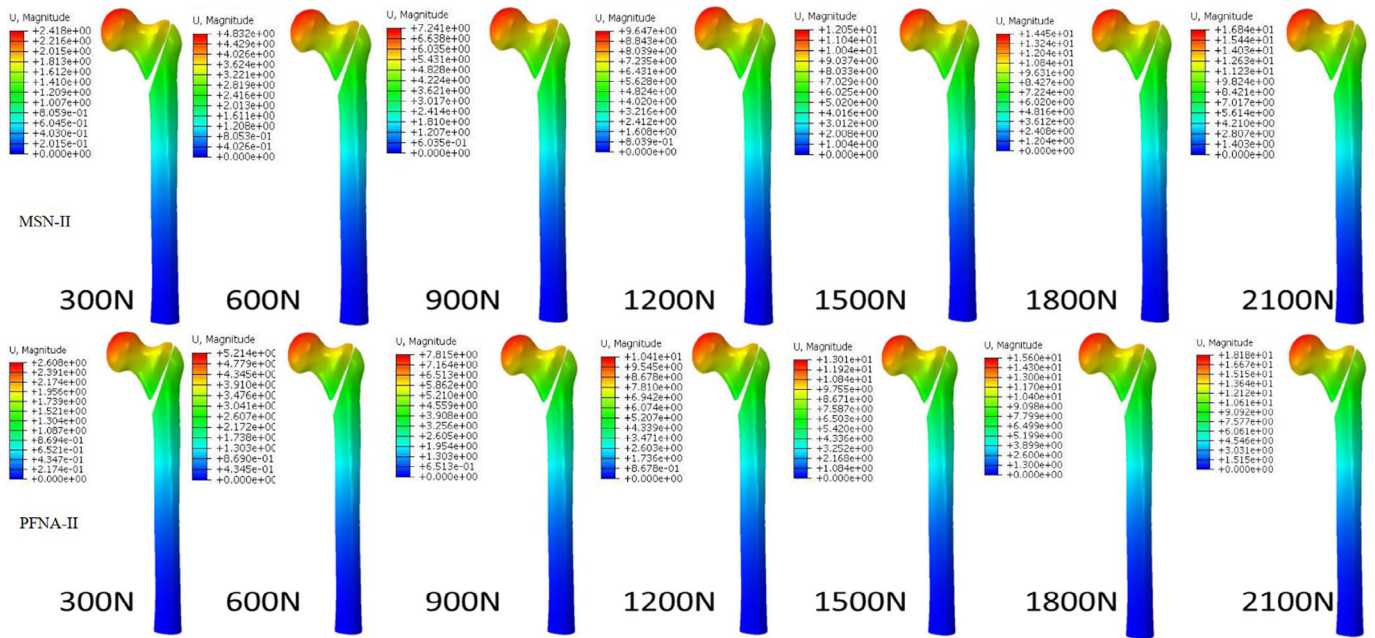
Fig. 9 Pressure cloud diagram of the displacement of proximal fragment in MSN-II and PFNA-II under different loads

TABLE 2 Statistical analysis of the comparison of biomechanical characteristics between the two groups				
Biomechanical characteristics	MSN-II	PFNA-II	t	p
Sliding distance of helical blade	0.37 ± 0.2	0.82 + 0.44	−4.774	0.003
Maximum stress of femur	393.7 ± 212.6	411.9 + 222.4	−4.911	0.003
Maximum stress of nail	734.5 ± 390.2	831.4 + 443.6	−4.796	0.003
Displacement of proximal fragment	9.6 ± 5.2	10.4 + 5.6	−4.917	0.003

compared with the PFNA-II group, and the difference was statistically significant ($t = -4.917$, $P < 0.05$). (Table 2).

Discussion

It was found that MSN-II had less sliding distance than PFNA-II in the fixation of medial comminuted intertrochanteric fracture by the finite element analysis. In addition, the maximum stress of femur, the maximum stress of nail and the displacement of proximal fragment in MSN-II group was less than that of PFNA-II group. Therefore, MSN-II may reduce the risk of implant failure by limiting sliding distance and resisting femur medialization.

Restriction Sliding and Cut out

Cut out is a common complication of intramedullary nailing, mainly related to the excess sliding of the helical blade or femoral medialization.[36] Goffin et al. found that the part of the femoral head with highest bone density was located in the middle and lower part of the femoral head,[37] and he suggested that the helical blade should be placed in the middle and lower part of the femoral neck, in order to resist the axial pressure to prevent cut out. Kwak et al. conducted a comparative study on Gamma3, Gamma 3 with U-shape blade and PFNA-II by

biomechanics, and found that PFNA-II and U-shape blade had better anti-rotation ability.[38] However, even if the blade is placed in the middle and lower 1/3 of the femoral head, the proximal fragment is prone to varus and the blade is cut out. That may be due to the excessive sliding and cutting during weight bearing. The modified MSN (MSN-II) blade, with the addition of a limited sliding groove and the removal of the upper blade which reduced the sliding distance and increasing varus resistance so that the risk of cut out is reduced. In this study, the sliding distance of the MSN-II blade in femoral neck was smaller than that of PFNA-II (Fig. 2), indicating that MSN-II achieved the purpose of avoiding excessive sliding. Meanwhile, less proximal fragment displacement of MSN-II (Fig. 9) also suggested that MSN-II has a better ability to resist varus. The stress concentration on the MSN-II helical blade was less than that of PFNA-II in the stress cloud diagram (Fig. 7) suggested that the stress distribution of the helical blade was dispersed because of the proximal triangular configuration. All of these lead to a reduced risk of cutting out or cutting through.

Medial Support and Coax Varus

Cephalomedullary nailing is the main treatment for intertrochanteric fracture, in which PFNA-II is the mainstream

implant, but the complications associated with PFNA-II are as high as 8%–40%,[39] among which the most common is coxa varus,[40] which is also the most serious complication. Once the varus occurs, the success rate of revision is less than 50%.[40] Coxa varus is caused by the comminution of the posteromedial cortex of the femur and the inability to maintain the medial femoral support structure. In addition, PFNA-II could not effectively restore the support of the femoral posteromedial and therefore could not resist coxa varus during weightbearing. That leads to the failure of secondary stability of fracture and the proximal fragment prone to varus. Not only PFNA-II, but existing hip implants are also unable to effectively reconstruct the medial support in an early minimally invasive way.[41] Therefore, many scholars added surgical incision during surgery and used steel wire or additional steel plate for fixation, but increased operative and anesthesia time resulted in more bleeding and increased risk of infection.[42] MSN-II can prevent coxa varus by simply adding medial support screws to fulfill the void between nail and femoral medial cortex without additional incision and forming support for the medial cortex of the proximal fragment. Moreover, the medial support screw is placed under the middle part of the helical blade to disperse the pressure on the helical blade. Part of the stress is transmitted to the distal femur where the bone cortex is thicker and stronger thereby reducing the stress of the helical blade hole in nail and the risk of implant fracture. In this study, the stress on the femur and the nail of MSN-II is smaller than that in PFNA-II (Figs 4 and 6), besides that, the stress on the medial of MSN-II nail is larger than that of PFNA-II and the stress in the proximal of MSN-II nail is less than that of PFNA-II in stress nephogram (Fig. 7) which mean the stress on the proximal femur has been transmitted to distal of nail. In the majority of cases, breakage occurs at the proximal aperture for the cervicocephalic screw.[43] The stress of the proximal aperture for the cervicocephalic screw decreases as the support screw disperses stress to the distal medial side of the nail. As a result of that, the risk of implant breakage is reduced and the pressure distribution between the long reamer and the intramedullary nail of MSN-II was higher than that in the PFNA group (see Fig. 7). In terms of proximal fragment displacement, the MSN-II was smaller than PFNA-II, which also suggested that the risk of coxa varus was lower than that of the PFNA-II in the posteromedial no support intertrochanteric fractures with MSN-II fixation after adjustment of fixation structure.

Potential Risk

The medial support screw did not increase the risk of fracture of the lateral femoral wall. The lateral femoral wall is the part of the lateral femoral cortex between the extensions of the superior and inferior femoral neck.[44] The medial support screw is located below this area. That is an increased risk of subtrochanteric fracture after femoral neck fixation with cannulated screws when the distal most screw is placed distal to the lesser trochanter.[45] Kim *et al.* found that peri-

implant atypical femoral fracture may develop through the screw hole at the subtrochanteric or diaphyseal area due to femoral fragility and stress riser effect of the implant.[46] In this study, concentration of stress was not in the femur around the supporting screw but the fracture site in the stress cloud map. Since the function of sliding compression was maintained in the design of MSN-II, such stress concentration can compress at the fracture end and accelerate fracture union. The stress of the lateral femoral cortex in MSN-II is higher than that in PFNA-II, but the stress was evenly distributed in the lateral and lateral cortex of the femur (Fig. 7). MSN-II does not have the same stress concentration around the proximal helical blade hole as PFNA-II and is therefore less at the risk of femoral fracture. That maybe since the support screw hole is in the cortical thick region rather than the gradient area of cortical thickness and the small diameter of the support screw which has little influence on the overall stability of the femur. Moreover, the stress of the helical blade hole is transmitted to the distal of the femur. All of the above conditions may be the reason why the support screws did not increase the risk of femoral fracture, however, the actual effect of MSN-II needs further clinical verification.

Strengths and Limitations

This study also has some limitations. First, this is simulated mechanical study even though.

simulate the gradual loading of the hip by applying different loads and more studies are needed to confirm this conclusion to ensure that it is not exaggerated. Second, Although the femur model was derived from an elderly woman with osteoporosis, we assumed that the femur was composed of homogeneous and elastic material, and that this homogeneity was sufficient for the purpose of comparing biomechanical properties.[47] So we believe that this study can still provide a reference for clinical treatment.

Conclusions

The sliding distance of helical blade in femoral neck, the maximum stress on the femur and nail, and the displacement of proximal fragment of MSN-II were less than those of PFNA-II in the treatment of unstable intertrochanteric fractures. Therefore MSN-II has better stability than PFNA-II and it may have the potential to avoid femur medialization and cut out. It might be an option in unstable trochanteric fractures because of its superiority in restricted sliding and medial support reconstruction.

Authors' Contributions

All authors had full access to the data in the study and take responsibility for the integrity of the data and the

References

1. Hung WW, Egol KA, Zuckerman JD, Siu AL. Hip fracture management: tailoring care for the older patient. JAMA. 2012;307(20):2185–94.

2. Long H, Cao R, Zhang H, Qiu Y, Yin H, Yu H, et al. Incidence of hip fracture among middle-aged and older Chinese from 2013 to 2015: results from a nationally representative study. Arch Osteoporos. 2022;17(1):48.

3. Bhandari M, Swiontkowski M. Management of acute hip fracture. N Engl J Med. 2017;377(21):2053–62.

4. Luo W, Fu X, Ma JX, Huang JM, Wu J, Ma XL. Biomechanical comparison of INTERTAN nail and Gamma3 nail for intertrochanteric fractures. Orthop Surg. 2020;12(6):1990–7.

5. Zhang H, Zhu X, Pei G, Zeng X, Zhang N, Xu P, et al. A retrospective analysis of the InterTan nail and proximal femoral nail anti-rotation in the treatment of intertrochanteric fractures in elderly patients with osteoporosis: a minimum follow-up of 3 years. J Orthop Surg Res. 2017;12(1):147.

6. Li J, Zhang L, Zhang H, Yin P, Lei M, Wang G, et al. Effect of reduction quality on post-operative outcomes in 31-A2 intertrochanteric fractures following intramedullary fixation: a retrospective study based on computerised tomography findings. Int Orthop. 2019;43(8):1951–9.

7. Seyhan M, Turkmen I, Unay K, Ozkut AT. Do PFNA devices and Intertan nails both have the same effects in the treatment of trochanteric fractures? A prospective clinical study. J Orthop Sci. 2015;20(6):1053–61.

8. Grønhaug KML, Dybvik E, Matre K, Östman B, Gjertsen JE. Intramedullary nail versus sliding hip screw for stable and unstable trochanteric and subtrochanteric fractures: 17,341 patients from the Norwegian hip fracture register. Bone Jt J. 2022;104-B(2):274–82.

9. Song H, Chang SM, Hu SJ, Du SC. Low filling ratio of the distal nail segment to the medullary canal is a risk factor for loss of anteromedial cortical support: a case control study. J Orthop Surg Res. 2022;17(1):27.

10. Ceynowa M, Zerdzicki K, Klosowski P, Pankowski R, Rocławski M, Mazurek T. The early intramedullary nail and the dynamic hip screw in femurs with a wide medullary canal. A biomechanical study of intertrochanteric fractures. Clin Biomech. 2020;71:201–7.

11. Chen SY, Chang SM, Tuladhar R, Wei Z, Xiong WF, Hu SJ. A new fluoroscopic view for evaluation of anteromedial cortex reduction quality during cephalomedullary nailing for intertrochanteric femur fractures: the 30° oblique tangential projection. BMC Musculoskelet Disord. 2020;21(1):719.

12. Song H, Chang SM, Hu SJ, Du SC, Xiong WF. Calcar fracture gapping: a reliable predictor of anteromedial cortical support failure after cephalomedullary nailing for pertrochanteric femur fractures. BMC Musculoskelet Disord. 2022;23(1):175.

13. Ehrnthaller C, Olivier AC, Gebhard F, Dürselen L. The role of lesser trochanter fragment in unstable pertrochanteric A2 proximal femur fractures—is refixation of the lesser trochanter worth the effort? Clin Biomech. 2017;42:31–7.

14. Lewis SR, Macey R, Lewis J, Stokes J, Gill JR, Cook JA, et al. Surgical interventions for treating extracapsular hip fractures in older adults: a network meta-analysis. Cochrane Database Syst Rev. 2022;2(2):CD013405.

15. Mao W, Ni H, Li L, He Y, Chen X, Tang H, et al. Comparison of Baumgaertner and Chang reduction quality criteria for the assessment of trochanteric fractures. Bone Jt Res. 2019;8(10):502–8.

16. Law GW, Wong YR, Yew AK, Choh ACT, Koh JSB, Howe TS. Medial migration in cephalomedullary nail fixation of pertrochanteric hip fractures: a biomechanical analysis using a novel bidirectional cyclic loading model. Bone Jt Res. 2019;8(7):313–22.

17. Law GW, Wong YR, Gardner A, Ng YH. Intramedullary nailing confers an increased risk of medial migration compared to dynamic hip screw fixation in unstable intertrochanteric hip fractures. Injury. 2021;52(11):3440–5.

18. Chapman T, Zmistowski B, Krieg J, Stake S, Jones CM, Levicoff E. Helical blade versus screw fixation in the treatment of hip fractures with cephalomedullary devices: incidence of failure and atypical "medial cutout". J Orthop Trauma. 2018;32(8):397–402.

19. Chinzei N, Hiranaka T, Niikura T, Tsuji M, Kuroda R, Doita M, et al. Comparison of the sliding and femoral head rotation among three different femoral head fixation devices for trochanteric fractures. Clin Orthop Surg. 2015;7(3):291–7.

20. Goto K, Murakami T, Saku I. Postoperative subtype P as a risk factor for excessive postoperative sliding of cephalomedullary nail in femoral trochanteric fractures in old patients: a case series of 263 patients using computed tomography analysis. Injury. 2022;53(6):2163–71.

21. Schopper C, Faschingbauer M, Moeller RT, Gebhard F, Duerselen L, Seitz A. Modified candy-package technique vs cerclage technique for refixation of the lesser trochanteric fragment in pertrochanteric femoral fractures. A biomechanical comparison of 10 specimens. Injury. 2020;51(8):1763–8.

22. Kulkarni SG, Babhulkar SS, Kulkarni SM, Kulkarni GS, Kulkarni MS, Patil R. Augmentation of intramedullary nailing in unstable intertrochanteric fractures using cerclage wire and lag screws: a comparative study. Injury. 2017;48(Suppl 2):S18–22.

23. Rehme J, Woltmann A, Brand A, von Rüden C. Does auxiliary cerclage wiring provide intrinsic stability in cephalomedullary nailing of trochanteric and subtrochanteric fractures? Int Orthop. 2021;45(5):1329–36.

24. Kang SJ, Bao FL, Huang DS, Jiang T, Hu YM, Li JM, et al. Percutaneous cerclage wiring combined with Cephalomedullary nailing for irreducible subtrochanteric fractures. Orthop Surg. 2021;13(6):1899–911.

25. Ceynowa M, Zerdzicki K, Klosowski P, Pankowski R, Rocławski M, Mazurek T. Cerclage cable augmentation does not increase stability of the fixation of intertrochanteric fractures. A biomechanical study. Orthop Traumatol Surg Res. 2021;107(6):103003.

26. Raina DB, Markevičiūtė V, Stravinskas M, Kok J, Jacobson I, Liu Y, et al. A new augmentation method for improved screw fixation in fragile bone. Front Bioeng Biotechnol. 2022;10:816250.

27. Yamamoto N, Ogawa T, Banno M, Watanabe J, Noda T, Schermann H, et al. Cement augmentation of internal fixation for trochanteric fracture: a systematic review and meta-analysis. Eur J Trauma Emerg Surg. 2022;48(3):1699–709.

28. Tang PF, Wang Y, Zhang BX, et al. PLAGH's Orthopaedic trauma surgery. Beijing: Peoples Military Medical Press; 2013. p. 314.

29. Li J, Han L, Zhang H, Zhao Z, Su X, Zhou J, et al. Medial sustainable nail versus proximal femoral nail antirotation in treating AO/OTA 31-A2.3 fractures: finite element analysis and biomechanical evaluation. Injury. 2019;50(3):648–56.

30. Nie S, Li M, Ji H, Li Z, Li W, Zhang H, et al. Biomechanical comparison of medial sustainable nail and proximal femoral nail antirotation in the treatment of an unstable intertrochanteric fracture. Bone Jt Res. 2020;9(12):840–7.

31. Nie SB, Zhao YP, Li JT, Zhao Z, Zhang Z, Zhang LC, et al. Medial support nail and proximal femoral nail antirotation in the treatment of reverse obliquity inter-trochanteric fractures (Arbeitsgemeinschaft fur Osteosynthesfrogen/orthopedic trauma association 31-A3.1): a finite-element analysis. Chin Med J. 2020;133(22):2682–7.

32. Li J, Tang S, Zhang H, Li Z, Deng W, Zhao C, et al. Clustering of morphological fracture lines for identifying intertrochanteric fracture classification with Hausdorff distance-based K-means approach. Injury. 2019;50(4):939–49.

33. Noor S, Pridham C, Fawcett T, Barclay M, Feng YT, Hassan O, et al. Finite element analysis modelling of proximal femoral fractures, including post-fixation periprosthetic fractures. Injury. 2013;44(6):791–5.

34. Goffin JM, Pankaj P, Simpson AH. A computational study on the effect of fracture intrusion distance in three- and four-part trochanteric fractures treated with gamma nail and sliding hip screw. J Orthop Res. 2014;32(1):39–45.

35. Nüchtern JV, Ruecker AH, Sellenschloh K, Rupprecht M, Püschel K, Rueger JM, et al. Malpositioning of the lag screws by 1- or 2-screw nailing systems for pertrochanteric femoral fractures: a biomechanical comparison of gamma 3 and intertan. J Orthop Trauma. 2014;28(5):276–82.

36. Bojan AJ, Jönsson A, Granhed H, Ekholm C, Kärrholm J. Trochanteric fracture-implant motion during healing—a radiostereometry (RSA) study. Injury. 2018;49(3):673–9.

37. Goffin JM, Pankaj P, Simpson AH, Seil R, Gerich TG. Does bone compaction around the helical blade of a proximal femoral nail anti-rotation (PFNA) decrease the risk of cut-out? A subject-specific computational study. Bone Jt Res. 2013;2(5):79–83.

38. Kwak DK, Kim WH, Lee SJ, Rhyu SH, Jang CY, Yoo JH. Biomechanical comparison of three different intramedullary nails for fixation of unstable Basicervical intertrochanteric fractures of the proximal femur: experimental studies. Biomed Res Int. 2018;2018:7618079–9.

39. Müller F, Doblinger M, Kottmann T, Füchtmeier B. PFNA and DHS for AO/OTA 31-A2 fractures: radiographic measurements, morbidity and mortality. Eur J Trauma Emerg Surg. 2020;46(5):947–53.

40. Min BW, Lee KJ, Oh JK, Cho CH, Cho JW, Kim BS. The treatment strategies for failed fixation of intertrochanteric fractures. Injury. 2019;50(7):1339–46.

41. Chang SM, Song DL, Ma Z, Tao YL, Chen WL, Zhang LZ, et al. Mismatch of the short straight cephalomedullary nail (PFNA-II) with the anterior bow of the femur in an Asian population. J Orthop Trauma. 2014;28(1):17–22.
42. Kim GM, Nam KW, Seo KB, Lim C, Kim J, Park YG. Wiring technique for lesser trochanter fixation in proximal IM nailing of unstable intertrochanteric fractures: a modified candy-package wiring technique. Injury. 2017;48(2):406–13.
43. Lambers A, Rieger B, Kop A, D'Alessandro P, Yates P. Implant fracture analysis of the TFNA proximal femoral nail. J Bone Jt Surg. 2019;101(9):804–11.
44. Haq RU, Manhas V, Pankaj A, Srivastava A, Dhammi IK, Jain AK. Proximal femoral nails compared with reverse distal femoral locking plates in intertrochanteric fractures with a compromised lateral wall; a randomised controlled trial. Int Orthop. 2014;38(7):1443–9.

45. Crump EK, Quacinella M, Deafenbaugh BK. Does screw location affect the risk of subtrochanteric femur fracture after femoral neck fixation? A biomechanical study. Clin Orthop Relat Res. 2020;478(4): 770–6.
46. Kim JW, Oh CW, Park KH, Oh JK, Yoon YC, Kim JK. Peri-implant atypical femoral fracture after nail or plate osteosynthesis [published online ahead of print, 2021 May 27]. J Orthop Sci. 2021;S0949-2658(21): 144–5.
47. Oken OF, Soydan Z, Yildirim AO, Gulcek M, Ozlu K, Ucaner A. Performance of modified anatomic plates is comparable to proximal femoral nail, dynamic hip screw and anatomic plates: finite element and biomechanical testing. Injury. 2011;42(10):1077–83.